minerals

MDPI

Article

Acid Resistance and Ion-Exchange Capacity of Natural Mixtures of Heulandite and Chabazite

Vladimer Tsitsishvili [1], Marinela Panayotova [2,*], Nato Mirdzveli [3], Nagima Dzhakipbekova [4], Vladko Panayotov [5], Nanuli Dolaberidze [3] and Manana Nijaradze [3]

[1] Department of Chemistry and Chemical Technologies, Georgian National Academy of Sciences, Tbilisi 0108, Georgia
[2] Department of Chemistry, University of Mining and Geology "St. Ivan Rilski", 1700 Sofia, Bulgaria
[3] Petre Melikishvili Institute of Physical and Organic Chemistry, I. Javakhishvili Tbilisi State University, Tbilisi 1086, Georgia
[4] Department of Chemistry and Pharmaceutical Industry, Mukhtar Auezov South Kazakhstan University, Shymkent City 160012, Kazakhstan
[5] Engineering Sciences Unit, Bulgarian Academy of Sciences, 1000 Sofia, Bulgaria
* Correspondence: marichim@mgu.bg; Tel.: +359-28060305

Abstract: The recovery and immobilization of metals from wastewater often occurs in an acidic environment that destroys the structure of adsorbents such as zeolites, which are porous crystalline aluminosilicates. The influence of hydrochloric acid solutions on the structure and properties of two natural mixtures of heulandite (HEU) and chabazite (CHA)—tuff from the Georgian Dzegvi-Tedzami deposit (HEU/CHA ≈ 8) and rock from the Kazakhstani deposit Chankanay (HEU/CHA ≈ 1)—was studied by the X-ray energy dispersion spectra and diffraction patterns, as well as by adsorption of water, benzene, and nitrogen methods. It was found that acid-mediated dealumination, decationization, dissolution, and changes in systems of micro- and mesopores depend on the nature and chemical composition of the initial zeolites. It is concluded that, under the influence of acid, (i) zeolite micropores become accessible to relatively large molecules and ions, and the surface area of the adsorbent increases; (ii) the volume of mesopores decreases, and pores with a diameter of less than 4 nm become predominant; (iii) in terms of the degree of dealumination and dissolution rate, Kazakhstani zeolite is more acid-resistant than Georgian heulandite; and (iv) Kazakhstani zeolite retains a high ion-exchange capacity in an acidic environment, while Georgian heulandite, treated with dilute hydrochloric acid solutions, uptakes relatively high amounts of valuable silver, copper, and zinc.

Keywords: heavy metals; wastewater; heulandite-clinoptilolite; chabazite; bactericidal metal ions exchanged zeolites

check for updates

Citation: Tsitsishvili, V.; Panayotova, M.; Mirdzveli, N.; Dzhakipbekova, N.; Panayotov, V.; Dolaberidze, N.; Nijaradze, M. Acid Resistance and Ion-Exchange Capacity of Natural Mixtures of Heulandite and Chabazite. *Minerals* **2023**, *13*, 364. https://doi.org/10.3390/min13030364

Academic Editor: Jorge César Masini

Received: 1 February 2023
Revised: 1 March 2023
Accepted: 2 March 2023
Published: 4 March 2023

Copyright: © 2023 by the authors. Licensee MDPI, Basel, Switzerland. This article is an open access article distributed under the terms and conditions of the Creative Commons Attribution (CC BY) license (https://creativecommons.org/licenses/by/4.0/).

1. Introduction

The use of zeolites for the recovery or immobilization of heavy metals [1,2], such as cadmium [3–10], chromium [3–5,8,11–14], nickel [3,5,8,15], copper [3,5–9,11,15], zinc [3,5–9,15], lead [5–9,15–19], manganese [4,20,21], cobalt [9,11], iron, and others [14,22–25], from wastewater is an important tool for protecting the environment, and a possible way to recover valuable metals from waste streams.

Zeolites are porous crystalline aluminosilicates, $M_nSi_xAl_nO_{2(n+x)}{\cdot}mH_2O$ ($M^+ = Na^+$, K^+, … $\frac{1}{2}Ca^{2+}$, $\frac{1}{2}Mg^{2+}$, …), built from alternating SiO_4 and AlO_4^- tetrahedrons forming open framework uniform structures with cages and channels, which have entrance windows with usual sizes up to 1 nm. Currently, 248 zeolite framework types describing natural and synthetic zeolites are known, in accordance with the data of the International Zeolite Association (IZA) [26]. The use of natural and synthetic zeolites is based on a combination of molecular sieve, sorption, ion-exchange, and catalytic properties, among

which an important role is played by the ability of zeolites to maintain ion-exchange reactions between external ions and metal ions, compensating for the negative charge of the aluminosilicate crystal framework.

Extraction of metals from wastewater often occurs in an acidic environment, causing dealumination of zeolites [27], resulting in a decrease in their ion exchange capacity, and therefore it is advisable to use acid-resistant zeolites.

In general, synthetic zeolites are more suitable for sequestering heavy metals in wastewater treatment [1–3,5,7–9,11,12,16,19,22,25], followed by modified zeolites [1,2,13,15,20,21,24], whereas natural ones, albeit very interesting and appealing from an environmental and economic perspective, exhibit the least sorption for a good number of heavy metals [1–4,6,14,17,18,20,23,24]. It is noted [2] that the high uniformity of the distribution in pore size, hydrophobicity/hydrophilicity, and the existence of a sole compensation cation in synthetic zeolites warrants their superior capacity for cation exchange in comparison to natural zeolites.

However, the modification of natural zeolites through various chemical treatments can improve their properties [27]. Thus, monocationic natural zeolites obtained by ion exchange modification have a sufficiently high ion exchange capacity [1,2,20,21,24]. It has been shown that treatment with bases and/or acids leads to the washing out of impurities that block pores, resulting in an increase in the cation exchange capacity [28].

The effect of acid treatment on the properties and structure of natural zeolites has been studied by different authors. Rožić et al. studied the dealumination and decationization of Croatian clinoptilolite tuff as a result of its treatment with 0.1 N HCl solution [29]. Akimkhan investigated the eventual changes in the Si/Al ratio in natural clinoptilolite due to its relatively long (24 h) treatment with HCl solutions (3 and 12 M) [30]. Wang and coworkers studied the influence of a HNO_3 solution treatment on the structure and properties of natural zeolite clinoptilolite [31]. Silva and coauthors studied the effect of a 24 h acid treatment (nitric, sulfuric, and hydrochloric—1.25 M, 1.43, and 0.97 M, respectively) on the properties of Australian zeolite clinoptilolite [32]. They concluded that the treatment with HCl led to the most pronounced changes in the pore size and surface area of the zeolite. However, most of the published studies used clinoptilolite, and a prolonged treatment time and/or higher concentrations of acids. Although natural chabazite also showed a high sorption capacity with respect to heavy metals [33,34], to the best of our knowledge, there are no studies on the effect of an acid treatment on the properties and structure of natural chabazite, as well as comparing both zeolites with respect to the effect of the acid treatment.

The aim of this study was to examine acid-mediated changes in the chemical composition, structure, and properties of heulandite-bearing tuff from the Rkoni plot of the Tedzami-Dzegvi deposit (Eastern Georgia) and zeolitic rock from the Chankanay deposit (Kazakhstan, Almaty region), both chosen for the fabrication of new zeolite filter materials for removing heavy metals and water disinfection. Our goal was not only to determine the acid resistance of the studied zeolites, but also to establish the acid treatment conditions that improve the performance properties, in particular, the ion exchange capacity. It is well known that Ag^+-, Cu^+-, and Zn^+-loaded zeolites (by ion exchange) possess bactericidal properties [35–38].

2. Materials and Methods

Heulandite-chabazite-containing tuff from the Rkoni plot of the Tedzami-Dzegvi deposit (Eastern Georgia) and zeolitic rock of the Chankanay deposit (Kazakhstan, Almaty region), containing heulandite and chabazite, were ground using a standard crusher, fractionated to the particle size of 1–1.4 mm or 14–16 mesh, washed with distilled water to remove clay impurities, and dried at a temperature of 95–100 °C. The main characteristics of rocks, according to the results of their study [39], are given in Table 1.

Table 1. Features of the studied Georgian (Rkoni) and Kazakhstani (Chankanay) zeolite-containing rocks.

Sample from	Rkoni	Chankanay
Zeolite phase content (%)	90	70
Empirical formula	$(Na_{0.25}K_{0.06}Ca_{0.19}Mg_{0.15})$ $[AlSi_{3.6}O_{9.2}]\cdot 3H_2O$	$(Na_{0.115}K_{0.079}Ca_{0.228}Mg_{0.175})$ $[AlSi_{2.96}O_{7.92}]$ $3H_2O$
HEU/CHA [1]	8	1
Framework impurity	$Ti_{0.005}$	$Ti_{0.009}$
Impurities per Al atom	$Fe_{0.2}$, $Ca_{0.14}$	$(SiO_2)_{\approx 1}$, $Fe_{0.33}$, $Ca_{0.17}$

[1] HEU—content of heulandite ($M_8(H_2O)_{24}[Al_8Si_{28}O_{72}]$), CHA—content of chabazite ($M_{12}(H_2O)_{40}[Al_{12}Si_{24}O_{72}]$).

According to these data, the Georgian sample can be identified as a sodium heulandite (Si/Al = 3.6) with a small admixture of chabazite, while the Kazakhstani sample is a mixture of heulandite and chabazite with a large admixture of quartz.

Acid treatment of samples with 0.5, 1.0, and 2.0 N HCl solutions was carried out by mixing 10 g of original zeolitic tuff with 100 mL of the solution in a shaking water bath (OLS26 Aqua Pro, Grant Instruments, US, linear mode) at 75 °C. This temperature was chosen as optimal due to the reproducibility of the results (control of temperature constancy throughout the acid treatment), as well as for comparison with the results of published works [29,40]. To achieve the maximum effect, acid treatment was carried out in three stages: the first stage lasted 1 h, the second stage lasted 2 h, and the third stage lasted 3 h. Each stage was followed by washing with distilled water until no Cl^- ions were detected in the washing water, by using a $AgNO_3$ solution. Acid treatment with dilute solutions (0.032, 0.16, and 0.32 N) was carried out at room temperature and for 2 h.

Ion exchange reactions were carried out in 1 N solutions of silver nitrate, copper, and zinc chlorides at a solid:liquid ratio of 1:10 at room temperature, with stirring for 6 h; the prepared samples were dried at 100–110 °C. Silver(I) nitrate $AgNO_3$, zinc(II) chloride $ZnCl_2$, and copper(II) chloride dihydrate $CuCl_2\cdot 2H_2O$ (p.a., obtained from Merck KGaA—Darmstadt, Germany) were used without any additional purification.

Chemical composition of samples was calculated from the X-ray energy dispersive spectra (XR-EDS) obtained from a high-performance scanning electron microscope JSM-6490LV (JEOL, Japan), equipped with an INCA Energy 350 XRED analyzer (Oxford Instruments). Powder X-ray diffraction (XRD) patterns were obtained from a diffractometer D8 Endeavor (Bruker, Germany) using the Cu-K_α line (λ = 0.154056 nm); the powder XRD patterns were recorded by scanning at a rate of 1°/min in the 2Θ range of 5° to 100°, with a 0.02° step. Sorption of water and benzene vapors was measured in static conditions at room temperature and constant pressure. Nitrogen adsorption/desorption isotherms were measured at 77 K using the ASAP 2020 Plus analyzer (Micromeritics, Norcross, GA, USA) on samples vacuum degassed at 350 °C, and data analysis was carried out using the Brunauer–Emmett–Teller (BET) and Barrett-Joyner-Halenda (BJH) models.

3. Results and Discussion

3.1. Chemical Composition of the Acid-Treated Samples

The chemical composition of the acid-treated samples indicates their dealumination and decationization. After the first stage of acid treatment (1 h), the degree of dealumination reached 87–92% of the final value obtained, as a result of the second stage of treatment (2 h); after the third stage (3 h), the chemical composition of the resulting product did not change. All results below refer to samples obtained from the three-stage process.

3.1.1. Dealumination

The results for the chemical composition of the studied materials (XR-EDS analysis) are given in Table 2, in terms of averaged empirical formulas of dehydrated zeolites, the Si/Al molar ratio, and degree of dealumination (DD), which is defined as the ratio of the aluminum content of the treated sample to the aluminum content of the original sample.

Table 2. Chemical composition of unit cell, Si/Al molar ratio, and degree of dealumination (DD) in original and acid-treated Georgian (Rkoni) and Kazakhstani (Chankanay) zeolites.

[HCl] (N) [1]	Rkoni			Chankanay		
	Empirical Formula	Si/Al	DD	Empirical Formula	Si/Al	DD
0	$(Na_{1.95}K_{0.47}Ca_{1.49}Mg_{1.17})[Al_{7.83}Si_{28.2}O_{72}]$	3.6	1.00	$(Na_{1.05}K_{0.72}Ca_{2.07}Mg_{1.6})[Al_{9.1}Si_{26.9}O_{72}]$	2.96	1.00
0.5	$(Na_{0.62}K_{0.67}Ca_{0.71}Mg_{0.47})[Al_{4.58}Si_{31.4}O_{72}]$	6.85	0.58	$(Na_{0.98}K_{0.82}Ca_{1.07}Mg_{1.25})[Al_{8.96}Si_{27.0}O_{72}]$	3.02	0.98
1.0	$(Na_{0.47}K_{0.4}Ca_{0.65}Mg_{0.46})[Al_{4.26}Si_{31.7}O_{72}]$	7.45	0.54	$(Na_{0.92}K_{0.84}Ca_{1.05}Mg_{1.12})[Al_{8.53}Si_{27.5}O_{72}]$	3.22	0.94
2.0	$(Na_{0.096}K_{0.5}Ca_{0.61}Mg_{0.26})[Al_{3.43}Si_{32.6}O_{72}]$	9.5	0.44	$(Na_{0.72}K_{0.90}Ca_{0.84}Mg_{0.76})[Al_{7.88}Si_{28.1}O_{72}]$	3.57	0.87

[1] [HCl]—concentration of the hydrochloric acid solution.

An increase in the Si/Al molar ratio from 3.6 to 9.5, and a decrease in the aluminum content to 44% of the original, indicates deep acid-mediated dealumination in the Georgian heulandite, while in the Kazakhstani zeolite, aluminum is not so significantly leached. A significant increase in the Si/Al ratio was observed by Akimkhan [30] for clinoptilolite treated with HCl solutions, but at higher a temperature (96–98 °C) and longer treatment time. Based on their data from FTIR analysis, Silva and coauthors [32] also concluded that clinoptilolite treated with a HCl solution leads to an increase in the Si/Al ratio.

3.1.2. Decationization

The acid treatment also results in strong decationization of the aluminum-rich Georgian and Kazakhstani samples, as shown in Figure 1, by a decrease in the total charge of the compensating ions Na^+, K+, Ca^{2+}, and Mg^{2+}, as well as the share of each of these cations in compensating the negative charge of the zeolite framework as they are leached and replaced in the framework by H^+.

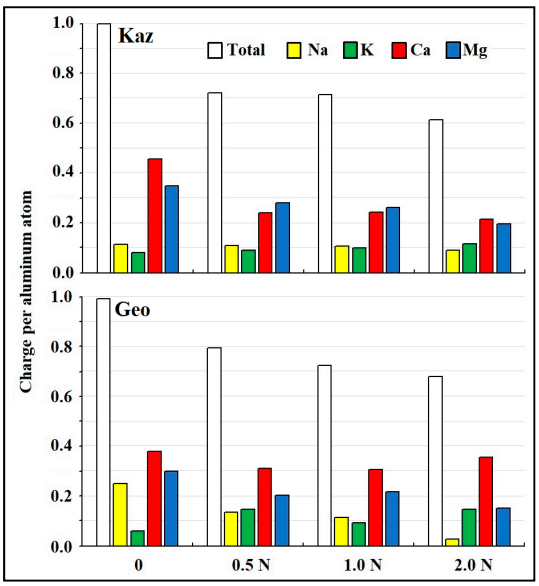


Figure 1. Cationic charge per Al atom of native (0) and acid-treated Georgian (Geo) and Kazakhstani (Kaz) zeolites.

In Georgian heulandite, the total charge monotonically decreases from ≈1 to ≈0.68 with increasing acid concentration. The contribution of Na^+ ions to compensate for the negative charge on aluminum atoms decreases, so that sodium is leached to the greatest extent (the sodium content decreased ≈9 times). The contribution of Mg^{2+} ions decreases more slowly (≈2 times), the contribution of Ca^{2+} ions changes insignificantly (−7%), and the contribution of K^+ ions increases nonmonotonically.

The degree of decationization of the Kazakhstani zeolite is also very high (from ≈1 to ≈0.62), but this process proceeds qualitatively differently. So, although the contribution of

sodium decreases, and the contribution of potassium increases, these changes are small (−20% and +30%, respectively), while the contribution of divalent cations, especially Ca^{2+}, decreases to the greatest extent (≈2 and ≈1.8 times for Ca^{2+} and Mg^{2+}, respectively).

Thus, in Georgian heulandite, the decationization mainly proceeds due to sodium ions, while calcium and, in particular, potassium are practically not involved in this process. This conclusion is consistent with the results of the study of decationization and dealumination of clinoptilolite tuff [29], where it was also found that natural clinoptilolite samples treated with HCl solutions exchanged mainly Na^+ ions, followed by Mg^{2+} and Ca^{2+} ions, whereas K+ ions from the clinoptilolite practically did not participate in an exchange process. However, our results do not correspond to the data of reference [40], which show that the removal of monovalent cations, such as Na^+ and K^+ ions, is insignificant for the temperatures of 25–100 °C, and changed little with acid concentration. This conclusion is more consistent with the decationization process in the Kazakhstani mixture of heulandite and chabazite, but the results are difficult to compare, since clinoptilolite with a high Si/Al ratio and a different cationic composition (Si/Al = 6.22, (Na+K) > Ca) was used in reference [40].

3.2. Structure of the Acid-Treated Samples

Structural changes of the studied materials are fixed by powder XRD patterns. The powder XRD pattern of Georgian heulandite shows no changes after treatment with a dilute HCl solution (0.5 N), but treatment with concentrated solutions leads to a change in the intensity of some peaks (see Figures 2 and 3). Thus, the intensity of the low angle peak at 2Θ = 9.85° (Miller indices *hkl* 020; d-spacing 8.98 Å) decreases with increasing acid concentration. The peak intensities at ≈22° (*hkl* 131, 400, 330; ≈4 Å) first increase (at 1.0 N), and then decrease (2.0 N), while the intensity of the weak peak at ≈28° (*hkl* −422 and/or −441; ≈3.15 Å) initially decreases, and then sharply increases with increasing the acid concentration to 2N.

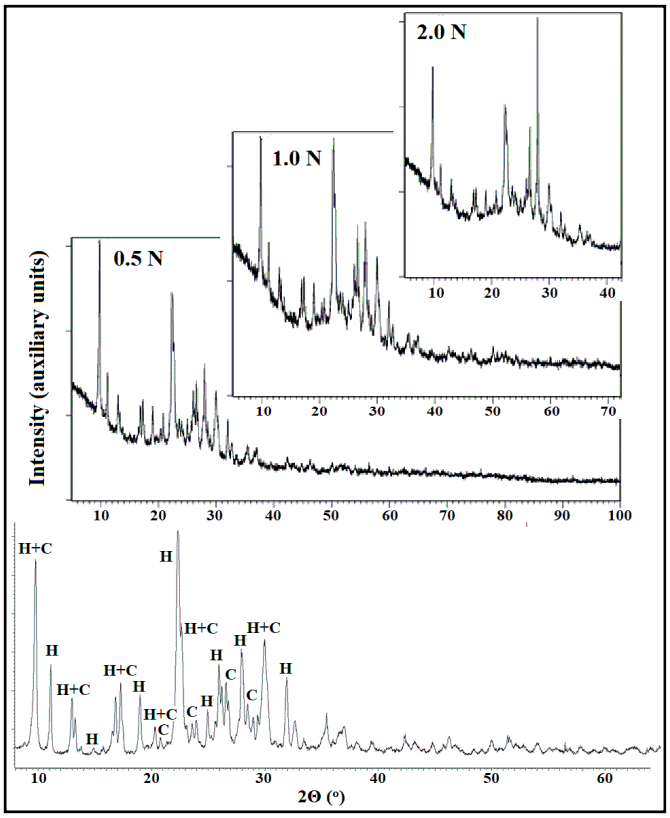


Figure 2. Powder XRD patterns of original (bottom left, H—peaks of heulandite, C—peaks of chabazite) and acid treated Georgian heulandite.

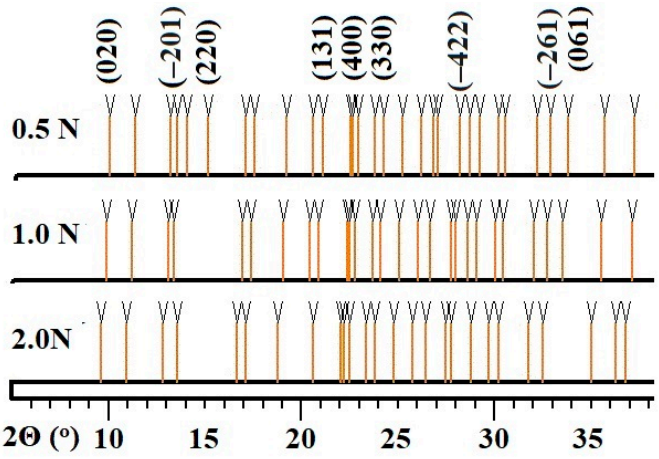


Figure 3. Schematic representation of powder XRD patterns of acid treated Georgian heulandite (numbers in parenthesis are Miller indices *hkl* of the most varying peaks).

In addition, some peaks decrease and disappear from the X-ray diffraction patterns with increasing acid concentration; this applies to peaks at 2Θ = 13° (*hkl* −201; 6.8 Å), 15° (*hkl* 220; ≈6 Å), and ≈33° (*hkl* −261 and/or 061; ≈2.8 Å), as schematically shown in Figure 3.

No line broadening is observed, so that the acid treatment does not cause amorphization of the sample. The overall intensity of the XRD pattern decreases slightly with increasing acid concentration, not correlating with the much greater weight loss resulting from the treatment, as shown in Table 3. Although the chemical compositions of the zeolites do not change in the third step of the acid treatment, there is still a slight weight loss, which indicates the gradual dissolution of the samples by the acid.

Table 3. Weight loss (%) from the acid treatment steps (1-2-3) of Georgian and Kazakhstani zeolites.

Zeolite Origin	From 0.5 N	From 1.0 N	From 2.0 N
Georgian	9.75–7.05–4.5	12.8–7.8–6.1	15.4–7.95–5.25
Kazakhstani	6.3–3.5–1.4	7.4–5.1–2.5	9.2–5.4–3.5

In a recent work [41], the amorphization of clinoptilolite recorded using XRD patterns was noted only after treatment of the zeolite with solutions with a high concentration of hydrochloric acid (5 and 10 N).

The same conclusions could be expected at high concentration of hydrochloric acid, based on a comparison of powder XRD patterns of the original and acid-treated samples of Kazakhstani zeolite (see Figure 4); since this zeolite is a mixture of heulandite and chabazite, the patterns are a superposition, and their detailed interpretation is quite difficult.

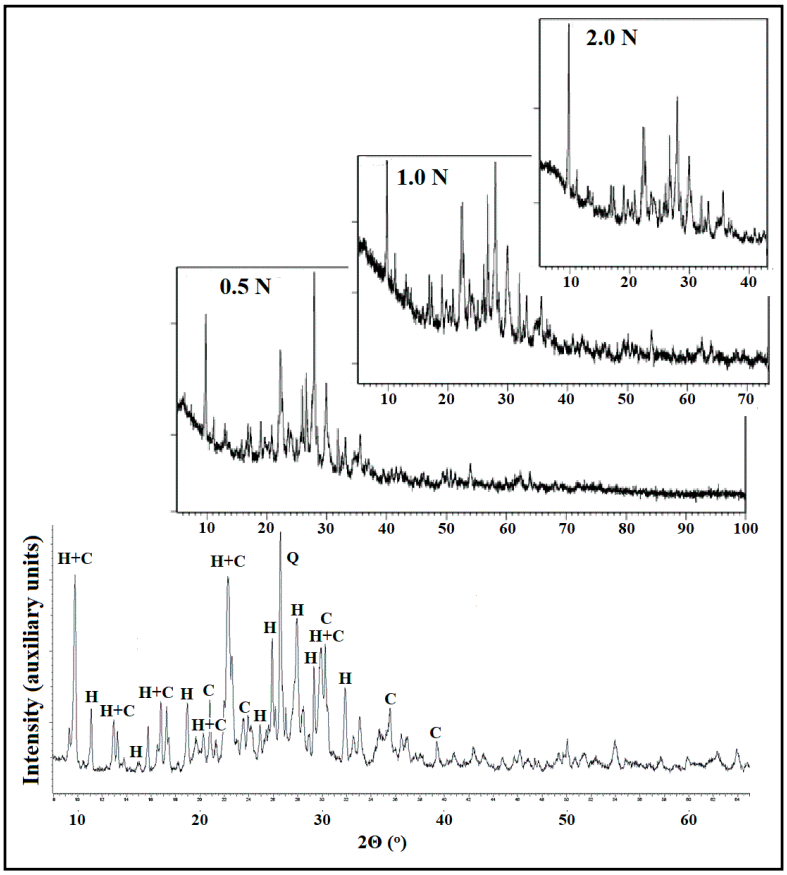


Figure 4. Powder XRD patterns of original (bottom left, H—peaks of heulandite, C—peaks of chabazite, Q—peak of quartz) and acid treated Kazakhstani zeolite.

3.3. Sorption Properties of the Acid-Treated Samples

Sorption properties carry information about micro- and mesoporous systems. The adsorption of small water molecules, with a kinetic molecular diameter of 0.266 nm, is a measure of the pore volume of high-aluminum zeolites due to their hydrophilicity. The adsorption capacity for water vapor at a relative pressure $p/p_o = 0.4$ reflects the micropore volume, and the adsorption capacity at saturated water vapor pressure ($p/p_o = 1.0$) reflects the total volume of micro-, meso-, and macropores [42].

The kinetic diameter of the benzene molecule is 0.585 nm, which significantly exceeds the sizes of micropores and channels in the studied zeolites. This non-polar molecule can be adsorbed only on the zeolite surface due to the presence of meso- and macropores; benzene adsorption capacity is a relative measure of surface area and its hydrophobicity.

The kinetic diameter of a nitrogen molecule N_2 (0.364 nm) is comparable to the size of the entrance windows in the chabazite crystal structure (eight-membered ring 0.38 × 0.38 nm [26]). In heulandite, a 10-membered ring (0.75 × 0.31 nm) and one of the 8-membered rings (0.47 × 0.28 nm) cannot accommodate a nitrogen molecule, which can pass only into one 8-membered ring (0.46 × 0.36 nm), which is due to the considerable flexibility of the framework [26].

3.3.1. Water and Benzene Sorption

The adsorption capacity of the studied zeolites, for water vapor at relative pressures of 0.4 and 1.0, as well as for benzene at a relative pressure of 1.0, is shown in Figure 5.

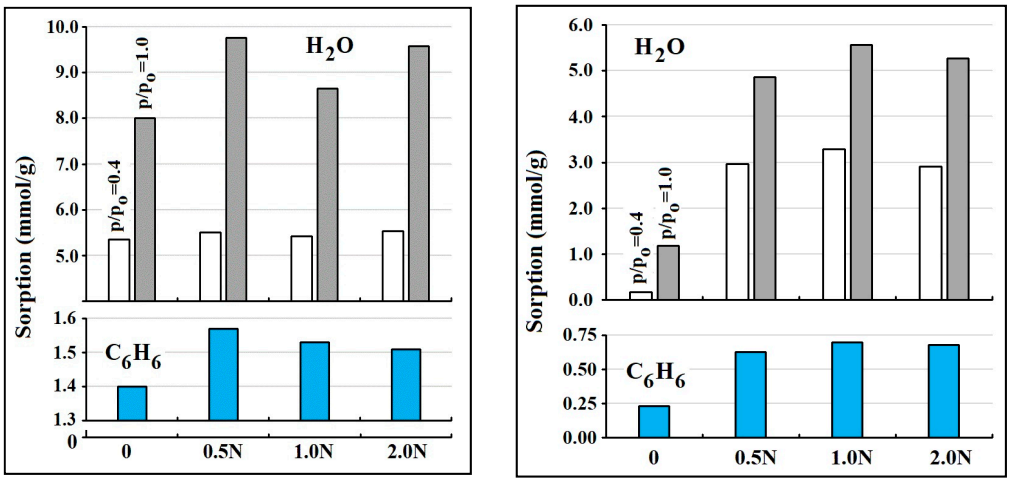


Figure 5. Water vapor (H_2O) and benzene (C_6H_6) adsorption capacity on original (0) and acid-treated samples of: (**a**) Georgian heulandite; (**b**) Kazakhstani zeolite.

According to the results obtained, for untreated Georgian heulandite, the volume of micropores accessible for water molecules is about 60% of the total pore volume; adsorption in the micropores practically does not change as a result of acid treatment, and the total adsorption in all the pores slightly increases. For untreated Kazakhstani zeolite, the volume of the micropores is only 10% of the total pore volume; adsorption in the micropores, as well as adsorption in all the pores, increases significantly after acid treatment; the volume of the micropores is increased ≈18 times and exceeds 60% of the total pore volume, as a result of treatment with a 1.0 N hydrochloric acid solution.

As a result of the study of high-silica zeolites [43–45], it was found that the strongest interaction of water molecules occurs with acidic protons bound to framework aluminum atoms H(Al), and the amount of adsorbed water is proportional to the content of framework aluminum. The zeolites studied by us, including acid-treated ones, have much lower values of the Si/Al ratio (3–9.5) than the samples studied in the indicated works (for example, Si/Al—35 [43] or Si/Al > 42 [44]), therefore, the effects described in [43–45] are not observed. Previously, Sano et al. [44] described the formation of mesopores in an acid-treated dealuminated synthetic zeolite, and this process apparently causes the observed increase in the total pore volume, which is especially characteristic of the Kazakhstani zeolite, but also occurs in Georgian heulandite.

Benzene adsorption changes insignificantly, but the results obtained indicate an increase in the hydrophobicity of the surfaces of both zeolites after acid treatment. More detailed information about the surface and mesopores was obtained by analyzing nitrogen adsorption-desorption isotherms.

3.3.2. Nitrogen Sorption

The porosity parameters of natural Georgian heulandite and its acid-treated forms (calculated on the basis of nitrogen adsorption-desorption isotherms—Figure S1) are shown in Table 4.

Table 4. Porosity parameters of Georgian heulandite and its acid-treated forms.

Concentration of HCl Solution (N)	0	0.5	1.0	2.0
Total volume of pores (cm^3/g) *	0.0895	0.109	0.1129	0.1256
Volume of micropores (cm^3/g)	0.00647	0.0782	0.0856	0.0889
BET surface area (m^2/g)	12.8	126.7	154.7	175.0
BJH desorption average pore diameter (nm)	17.2	13.1	11.6	11.1

* The total volume of pores with a diameter less than 200 nm.

Both the volume of micropores accessible to nitrogen molecules at p/p_0 = 0.4 and the surface area (calculated using the BET model) increase sharply for samples treated with acid, and continue to increase with increasing acid concentration, while the total pore volume, according to the number of molecules adsorbed at saturated vapor pressure, varies nonmonotonically with changes in acid concentration. The total pore volume increases monotonically with increasing acid concentration, while the diameter of nanosized pores, calculated using the BJH model, decreases abruptly. However, little depends on the acid concentration, indicating that acid treatment affects not only the heulandite micropore system, but also the mesopores existing in the sample.

The pore size distribution curve volume vs. pore diameter V(D) and differential dV/dD curve calculated by the BJH model for Georgian heulandite and its acid-treated forms are shown in Figure 6.

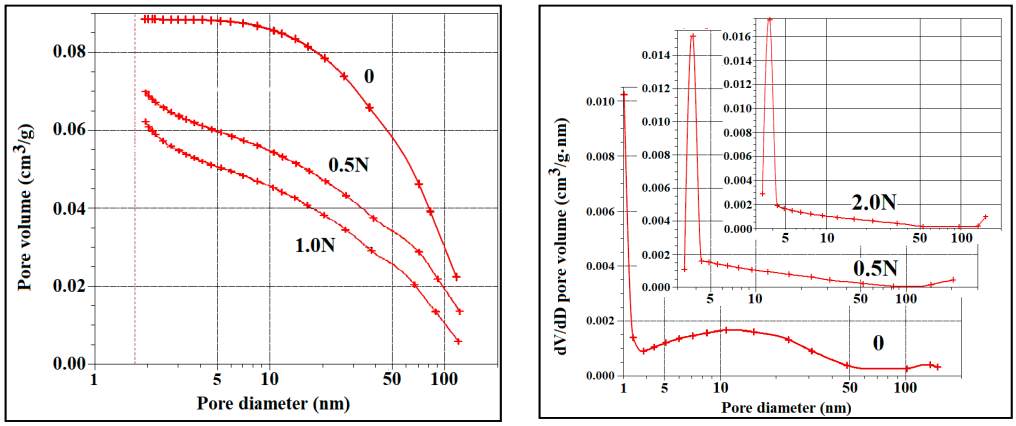


Figure 6. Pore size distribution curves calculated by the BJH model for Georgian heulandite and its acid-treated forms: (**a**) volume V vs. pore diameter D; (**b**) differential curve dV/dD.

As the pore size distribution curve V(D) shows, the volume of mesopores decreases as a result of acid treatment; according to the differential curve dV/dD, the maximum at ≈12 nm disappears, but a sharp maximum appears at ≈4 nm. Taking into account the, albeit small, increase in the total pore volume with increasing acid concentration, it can be concluded that after acid treatment, small in size, up to 4 nm, pores become predominant in the mesopore system of Georgian heulandite.

Akimkhan [30] observed no increase in the total pore volume when clinoptilolite was treated at room temperature with a 3 M HCl solution for 24 h; the increase was about two times when the acid was 12 M, and over three times when the acid treatment was at 96–98 °C. Silva and coworkers [32] found that HCl treatment decreased the zeolite pore diameter about 2.5 times, and increased the surface area approximately 16 times.

In a recent work by Çakicioğlu-Özkan and Becer [41], it was noted that in the studied original clinoptilolite, the volume of micropores accessible to nitrogen was only 0.005 cm^3/g, which the authors attributed to the blocking of most of the pores by cations, considered

as impurities. With an increase in the concentration of HCl in the solution, the volume of micropores increased by more than 12 times, up to 0.064 cm^3/g for a 3 N HCl solution, but with further increase in the acid concentration, it decreased. The outer surface area of the HCl-treated samples gradually increased with increasing the Si/Al ratio from 3 m^2/g, and reached a maximum of 33 m^2/g after soaking in a 10 N solution [41].

The values of micropore volume and surface area obtained by us for original and acid-treated heulandites are much higher than reported in [41], but the general tendencies of their change with increasing acid concentration are the same. The authors of [41] also processed data in the region of low relative pressures ($p/p_0 < 0.1$) using the Dubinin-Astakhov equation ($W = W_0 exp\{-[RTln(p_0/p)/E]^n\}$, where W_0 is total weight adsorbed, E is the characteristic energy, R—gas constant, T—temperature) and obtained fractal values of the heterogeneity parameter n for acid-treated samples, while the experimental data obtained by us are ideally described by the simple BET equation ($W = W_0[1 - (p/p_0)]$), at least up to pressures $p/p_0 = 0.08$. The pore size distributions were not calculated in [41].

The porosity parameters of natural Kazakhstani zeolite and its acid-treated forms (calculated on the basis of nitrogen adsorption-desorption isotherms—Figure S2), are shown in Table 5. As in Georgian heulandite, the quantity of nitrogen molecules adsorbed in micropores and the BET surface area increase sharply for samples treated with acid, and continue to increase with increasing acid concentration. Total pore volume, on the contrary, first increases and then decreases with increasing acid concentration; the diameters of nanosized pores calculated by the BJH model decrease monotonically.

Table 5. Porosity parameters of Kazakhstani zeolite and its acid-treated forms.

Concentration of HCl Solution (N)	**0**	**0.5**	**1.0**	**2.0**
Total volume of pores (cm^3/g) *	0.0732	0.0881	0.0735	0.0686
Volume of micropores (cm^3/g)	0.00152	0.0098	0.0189	0.0209
BET surface area (m^2/g)	2.75	20.0	38.0	44.9
BJH desorption average pore diameter (nm)	24.3	15.4	12.2	13.8

* The total volume of pores with a diameter less than 200 nm.

The differences in the systems of mesopores of Georgian and Kazakhstani zeolites should be noted: according to the pore size distribution V(D) and dV/dD curves calculated by the BJH model, using adsorption isotherms measured on original and acid-treated Kazakhstani zeolite and shown in Figure 7, the dV/dD curve for native zeolite from the Chankanay deposit has two maxima, at ≈6 and 60 nm.

The pore size distribution V(D) curves show that the volume of mesopores increases after treatment with a diluted (0.5 N) HCl solution, but decreases after treatment with concentrated solutions. The maximum of the differential curve dV/dD at ≈6 nm shifts to ≈4 nm, and the maximum at ≈60 nm disappears.

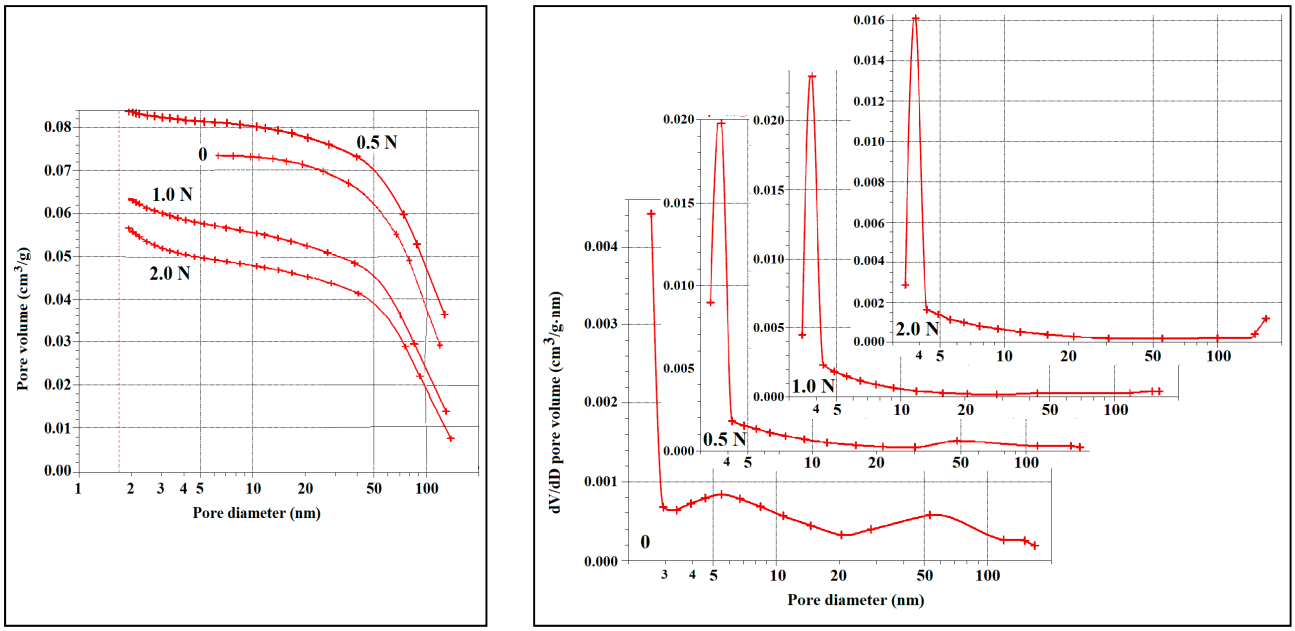


Figure 7. Pore size distribution curves calculated by the BJH model for Kazakhstani zeolite and its acid-treated forms: (**a**) volume V vs. pore diameter D; (**b**) differential curve dV/dD.

3.4. Effect of Dilute Solutions on the Porosity and Ion-Exchange Properties of Georgian Heulandite

The chemical composition of the ion-exchanged samples determines their cation exchange capacity. The cation exchange capacity (CEC) of the original and acid-treated samples was calculated from XR-EDS data, as the number of ionogenic groups of the ion exchanger entirely converted to the H^+ form, and expressed in milliequivalents per gram; the results are shown in Table 6, and the dependence of the obtained CEC values on the molar ratio Si/Al is shown in Figure 8.

Table 6. Cation exchange capacity (CEC, mEq/g) of the original and acid-treated samples.

Concentration of HCl Solution (N)	0	0.5	1.0	2.0
Georgian heulandite	3.03	1.90	1.78	1.46
Kazakhstani zeolite	3.43	3.38	3.25	3.05

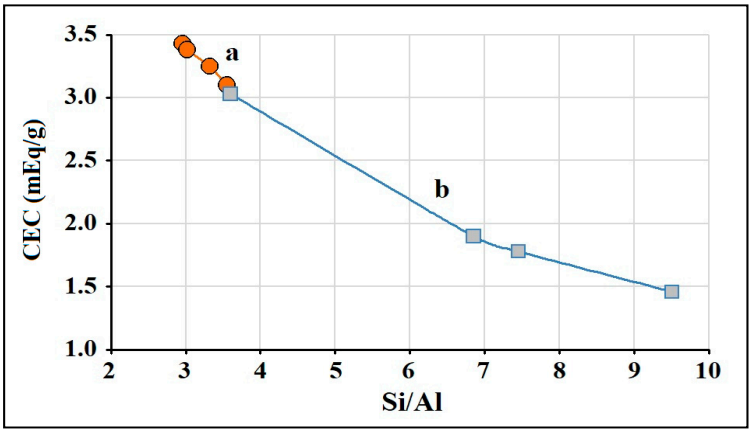


Figure 8. Dependence of the CEC on the Si/Al molar ratio, calculated for Kazakhstani zeolite (a) and Georgian heulandite (b).

The ion-exchange capacity of Kazakhstani zeolite remains at a high level of ≈3.4 mEq/g after treatment with a 0.5 N hydrochloric acid solution, which provides the access of large metal ions to the cages and channels of the zeolite, as well as a sufficiently large surface area (up to 20 m^2/g). For heulandite-bearing tuff, the ion-exchange capacity decreases significantly, which is associated with a higher degree of dealumination of this sample. In this regard, acid treatment was carried out under milder conditions (room temperature, 2 h), using more dilute solutions in the concentration range of 0.032–0.32 N.

The samples thus treated were subjected to ion exchange in solutions of silver nitrate and chlorides of copper and zinc. X-ray diffraction patterns of ion-exchanged samples confirm the preservation of the zeolite structure. The characteristics of the micro- and mesoporous systems of the acid-treated heulandites, and the chemical compositions of the exchanged samples, are shown in Table 7.

Table 7. Porosity parameters of acid-treated Georgian heulandite and chemical compositions of silver-, copper-, and zinc-exchanged forms.

Concentration of HCl Solution (N)	**0.032**	**0.16**	**0.32**
Total volume of pores (cm^3/g)	0.090	0.094	0.104
Volume of micropores (cm^3/g)	0.010	0.025	0.049
BET surface area (m^2/g)	19.6	49.8	87.5
BJH desorption pore diameter (nm)	17.0	16.2	15.4
Empirical formula of Ag-exchanged samples	$Ag_{0.46}(Na,K,Ca,Mg)_{0.54}[AlSi_{3.75}O_{9.5}]$	$Ag_{0.5}(Na,K,Ca,Mg)_{0.5}[AlSi_{4.6}O_{11.2}]$	$Ag_{0.42}(Na,K,Ca,Mg)_{0.57}[AlSi_{5.5}O_{13}]$
Silver content (mg/g, mmol/g)	122	117	90
	1.1	1.1	0.82
Empirical formula of Cu-exchanged samples	$Cu_{0.36}(Na,K,Ca,Mg)_{0.27}[AlSi_{3.9}O_{9.8}]$	$Cu_{0.4}(Na,K,Ca,Mg)_{0.18}[AlSi_{4.8}O_{11.6}]$	$Cu_{0.35}(Na,K,Ca,Mg)_{0.27}[AlSi_{5.6}O_{13.2}]$
Copper content (mg/g, mmol/g)	60	58.5	46
	0.95	0.92	0.72
Empirical formula of Zn-exchanged samples	$Zn_{0.16}(Na,K,Ca,Mg)_{0.67}[AlSi_{3.8}O_{9.6}]$	$Zn_{0.18}(Na,K,Ca,Mg)_{0.62}[AlSi_{4.7}O_{11.4}]$	$Zn_{0.15}(Na,K,Ca,Mg)_{0.67}[AlSi_{5.6}O_{13.2}]$
Zinc content (mg/g, mmol/g)	28	27	20
	0.43	0.42	0.31

Compared to the untreated sample, which retains only 0.62, 0.54, and 0.22 mmol/g of silver, copper, and zinc, respectively, the largest amount of metals is immobilized by heulandites treated with dilute solutions of hydrochloric acid (0.032–0.16 N); with an increase in acid concentration, the specific amount of embedded metals in the samples decreases (for example, to only 0.24 mmol/g for silver in zeolite treated with a 2N HCl solution), due to dealumination occurring as a result of the acid treatment. Table 7 presents the data on zeolites, which is interesting from an application point of view.

The incorporation of silver ions Ag^+ into the microporous structure of heulandite occurs rather easily; the introduction of bivalent copper ions—Cu^{2+} and zinc ions—Zn^{2+}, despite their smaller diameter, is difficult.

This phenomenon is likely associated with different geometry and energy characteristics of the hydration of ions entering the micropores of the zeolite. The diameter of the hydrated studied ions, in any case, exceeds the size of the entrance window, and ions cannot pass into the micropores. The dehydration energy depends on the number of water molecules in the complex, and it should be taken into account that the hydrated silver(I) ion ($Ag(H_2O)_4^+$) includes four water molecules arranged in a linearly distorted tetrahedron,

whereas the hydrated copper(II) and zinc(II) ions ($M(H_2O)_6^{2+}$) include six water molecules located at the vertices of the regular octahedron [46].

The content of immobilized metals is ≈60, ≈75, and ≈40% of the maximum values calculated from the ion exchange isotherms obtained on Turkish clinoptilolite [47] for silver, copper, and zinc, respectively. In [48], it is shown that acid-treated clinoptilolite adsorbs more zinc ions than untreated clinoptilolite, but the ion-exchange capacity of these samples, with respect to other metals, has not been studied.

Acid-treated Georgian heulandite exhibits a higher uptake of copper and zinc than sedimentary clinoptilolite from the Serbian field Zlatokop (0.41 and 0.225 mmol/g of Cu and Zn, respectively [49]); silver uptake is higher than that of natural clinoptilolite (0.84 mmol/g [50]), which is used for the combined disinfection and heavy metal purification of water streams. The achieved uptake of silver, copper, and zinc by acid-treated Georgian heulandite is much higher than that described for the clinoptilolite-bearing tuff of the Iranian Semnan deposit (0.24, 0.28, and 0.24 mmol/g of Ag, Cu, and Zn, respectively [51]), which improves the prospect to remove and concentrate these valuable metals from wastewater.

4. Conclusions

Taking into account the results of studying the effect of acid treatment on the structure and properties of two natural mixtures of heulandite and chabazite, the following conclusions can be drawn:

1. Treatment of the Georgian heulandite-bearing tuff of the Rkoni plot of the Dzegvi-Tedzami deposit with hydrochloric acid solutions leads to significant dealumination and decationization with sodium washout, while the Kazakhstani zeolitic rock of the Chankanay deposit, containing heulandite and chabazite in equal amounts, is much more acid-resistant, but it also undergoes significant decationization with calcium and magnesium washout;
2. Solutions of hydrochloric acid gradually dissolve the zeolite microporous crystal structure without its amorphization; the dissolution rate of Kazakhstani zeolite is much lower, especially in dilute solutions, than that of Georgian heulandite;
3. Heulandite micropores are, in any case, accessible to small water molecules; in Kazakhstani zeolite, they become accessible only after acid treatment. The acid treatment also leads to a slight increase in surface hydrophobicity for both samples;
4. Low-temperature nitrogen adsorption-desorption isotherms show an acid-mediated sharp increase of adsorption in the micropores and of the BET surface area, as well as a decrease in the specific volume and average diameter of the mesopores;
5. Treatment of Kazakhstani zeolite with a dilute solution of hydrochloric acid (up to 0.5 N) provides the access of large metal ions to the micropores of the zeolite, while maintaining a high ion-exchange capacity; Georgian heulandite treated with more dilute solutions (0.032–0.16 N) retains its ion-exchange capacity and exhibits a high ability to uptake valuable silver, copper, and zinc ions (up to 122, 60, and 28 mg/g, respectively), making increased acidity of the zeolite processing solution impractical.

Supplementary Materials: The following supporting information can be downloaded at: https://www.mdpi.com/article/10.3390/min13030364/s1, Figure S1: N2 adsorption-desorption isotherms on Georgian heulandite and its acid-treated forms. Figure S2: N2 adsorption-desorption isotherms on Kazakhstani zeolite and its acid-treated forms.

Author Contributions: Conceptualization, V.T.; investigation, N.M. and N.D. (Nagima Dzhakipbekova) and M.N.; methodology, M.P., V.P. and N.D. (Nanuli Dolaberidze); project administration, N.M. All authors have read and agreed to the published version of the manuscript.

Funding: This research was funded by the International Science and Technology Center (ISTC), grant number GE-2506 "Scientific substantiation of the possibility of creating new bactericidal zeolite filter materials for purification-decontamination of water from various sources".

Data Availability Statement: Data is contained within the article and Supplementary Material.

Conflicts of Interest: The authors declare no conflict of interest.

References

1. Yuna, Z. Review of the natural, modified, and synthetic zeolites for heavy metals removal from wastewater. *Environ. Eng. Sci.* **2016**, *33*, 443–454. [CrossRef]
2. de Magalhães, L.F.; da Silva, G.R.; Peres, A.E.C. Zeolite Application in Wastewater Treatment. *Adsorpt. Sci. Technol.* **2022**, *2022*, 4544104. [CrossRef]
3. Alvarez-Ayuso, E.; Garcia-Sanchez, A.; Querol, X. Purification of metal electroplating waste waters using zeolites. *Water Res.* **2003**, *37*, 4855–4862. [CrossRef] [PubMed]
4. Dal Bosco, S.M.; Jimenez, R.S.; Carvalho, W.A. Removal of toxic metals from wastewater by Brazilian natural scolecite. *J. Colloid Interf. Sci.* **2005**, *281*, 424–431. [CrossRef]
5. Ibrahim, H.S.; Jamil, T.S.; Hegazy, E.Z. Application of zeolite prepared from Egyptian kaolin for the removal of heavy metals: II. Isotherm models. *J. Hazard. Mat.* **2010**, *182*, 842–847. [CrossRef] [PubMed]
6. Batjargal, T.; Yang, J.-S.; Kim, D.-H.; Baek, K. Removal characteristics of Cd(II), Cu(II), Pb(II), and Zn(II) by natural Mongolian zeolite through batch and column experiments. *Separ. Sci. Technol.* **2011**, *46*, 1313–1320. [CrossRef]
7. Xie, W.-M.; Zhou, F.-P.; Bi, X.-L.; Chen, D.-D.; Li, J.; Sun, S.-Y.; Liu, J.-Y.; Chen, X.-Q. Accelerated crystallization of magnetic 4A-zeolite synthesized from red mud for application in removal of mixed heavy metal ions. *J. Hazard. Mat.* **2018**, *358*, 441–449. [CrossRef]
8. Bai, S.; Chu, M.; Zhou, L.; Chang, Z.; Zhang, C.; Liu, B. Removal of heavy metals from aqueous solutions by X type zeolite prepared from combination of oil shale ash and coal fly ash. *Energ. Sourc. Part A* **2022**, *44*, 5113–5123. [CrossRef]
9. Joseph, I.V.; Tosheva, L.; Doyle, A.M. Simultaneous removal of Cd(II), Co(II), Cu(II), Pb(II), and Zn(II) ions from aqueous solutions via adsorption on FAU-type zeolites prepared from coal fly ash. *J. Environ. Chem. Eng.* **2020**, *8*, 103895. [CrossRef]
10. Dosa, M.; Grifasi, N.; Galletti, C.; Fino, D.; Piumetti, M. Natural zeolite clinoptilolite application in wastewater treatment: Methylene blue, zinc and cadmium abatement tests and kinetic studies. *Materials* **2022**, *15*, 8191. [CrossRef]
11. Hui, K.S.; Chao, C.Y.; Kot, S.C. Removal of mixed heavy metal ions in wastewater by zeolite 4A and residual products from recycled coal fly ash. *J. Hazard. Mat.* **2005**, *127*, 89–101. [CrossRef] [PubMed]
12. Covarrubias, C.; García, R.; Arriagada, R.; Yánez, J.; Garland, M.T. Cr(III) exchange on zeolites obtained from kaolin and natural mordenite. *Micropor. Mesopor. Mat.* **2006**, *88*, 220–231. [CrossRef]
13. Zeng, Y.; Woo, H.; Lee, G.; Park, J. Adsorption of Cr (VI) on hexadecylpyridinium bromide (HDPB) modified natural zeolites. *Micropor. Mesopor. Mat.* **2010**, *130*, 83–91. [CrossRef]
14. Zanin, E.; Scapinello, J.; de Oliveira, M.; Rambo, C.L.; Franscescon, F.; Freitas, L.; de Mello, J.M.M.; Fiori, M.A.; Oliveira, V.; Magro, J.D. Adsorption of heavy metals from wastewater graphic industry using clinoptilolite zeolite as adsorbent. *Process Saf. Environ.* **2017**, *105*, 194–200. [CrossRef]
15. Huang, F.-C.; Han, Y.-L.; Lee, C.-K.; Chao, H.-P. Removal of cationic and oxyanionic heavy metals from water using hexadecyltrimethylammonium-bromide-modified zeolite. *Desalin. Water Treat.* **2016**, *57*, 17870–17879. [CrossRef]
16. Shariatinia, Z.; Bagherpour, A. Synthesis of zeolite NaY and its nanocomposites with chitosan as adsorbents for lead(II) removal from aqueous solution. *Powder Technol.* **2018**, *338*, 744–763. [CrossRef]
17. Xing, P.; Wang, C.; Ma, B.; Chen, Y. Removal of Pb(II) from aqueous solution using a new zeolite-type absorbent: Potassium ore leaching residue. *J. Environ. Chem. Eng.* **2018**, *6*, 7138–7143. [CrossRef]
18. Budianta, W.; Ardiana, A.; Andriyani, N. The removal of lead by natural zeolite. *E3S Web Conf.* **2020**, *200*, 06012. [CrossRef]
19. Jangkorn, S.; Youngme, S.; Praipipat, P. Comparative lead adsorptions in synthetic wastewater by synthesized zeolite A of recycled industrial wastes from sugar factory and power plant. *Heliyon* **2022**, *8*, e09323. [CrossRef]
20. Taffarel, S.R.; Rubio, J. On the removal of Mn^{2+} ions by adsorption onto natural and activated Chilean zeolites. *Miner. Eng.* **2009**, *22*, 336–343. [CrossRef]
21. Taffarel, S.R.; Rubio, J. Removal of Mn^{2+} from aqueous solution by manganese oxide coated zeolite. *Miner. Eng.* **2010**, *23*, 1131–1138. [CrossRef]
22. Bahaz, H.; Hadj Seyd, A.; Moulai, K.; Aggoun, M.S. Removal of heavy metals from an industrial effluent by synthesized zeolite: Case of Bounoura industrial zone. *Leban. Sci. J.* **2020**, *21*, 80–94. Available online: https://applications.emro.who.int/imemrf/322/Lebanese-Sci-J-2020-21-1-80-94-eng.pdf (accessed on 1 March 2023).
23. Eremin, O.V.; Epova, E.S.; Filenko, R.; Rusal, O.S.; Bychinsky, V.A. Use of zeolite rocks in metal recovery from mine water. *J. Min. Sci.* **2017**, *53*, 915–924. [CrossRef]
24. Ćurković, L.; Cerjan-Stefanović, Š.; Filipan, T. Metal ion exchange by natural and modified zeolites. *Water Res.* **1997**, *31*, 1379–1382. [CrossRef]
25. Iqbal, A.; Sattar, H.; Haider, R.; Munir, S. Synthesis and characterization of pure phase zeolite 4A from coal fly ash. *J. Clean. Prod.* **2019**, *219*, 258–267. [CrossRef]
26. Baerlocher, C.; McCusker, L.B. Database of Zeolite Structures. Available online: http://www.iza-structure.org/databases/ (accessed on 1 March 2023).

27. Szostak, R. Secondary synthesis methods. In *Introduction to Zeolite Science and Practice*; van Bekkum, H., Flanigen, E.M., Jacobs, P.A., Jansen, J.C., Eds.; Elsevier: Amsterdam, The Netherlands, 2001; pp. 261–297. [CrossRef]
28. Wang, S.; Peng, Y. Natural zeolites as effective adsorbents in water and wastewater treatment. *Chem. Eng. J.* **2010**, *156*, 11–24. [CrossRef]
29. Rozić, M.; Cerjan-Stefanović, S.; Kurajica, S.; Maeefat, M.R.; Margeta, K.; Farkas, A. Decationization and dealumination of clinoptilolite tuff and ammonium exchange on acid-modified tuff. *J. Colloid Interface Sci.* **2005**, *284*, 48–56. [CrossRef]
30. Akimkhan, A.M. Structural and ion-exchange properties of natural zeolite. In *Ion Exchange Technologies*; Kilislioglu, A., Ed.; IntechOpen: London, UK, 2012; pp. 261–282. [CrossRef]
31. Wang, C.; Cao, L.; Huang, I. Influences of acid and heat treatments on the structure and water vapor adsorption property of natural zeolite. *Surf. Interface Anal.* **2017**, *49*, 1249–1255. [CrossRef]
32. Silva, M.; Lecus, A.; Lin, Y.T.; Corrao, J. Tailoring natural zeolites by acid treatments. *J. Mater. Sci. Chem. Eng.* **2019**, *7*, 26–37. [CrossRef]
33. Pansini, M.; Colella, C. Dynamic data on lead uptake from water by chabazite. *Desalination* **1990**, *78*, 287–295. [CrossRef]
34. Torracca, E.; Galli, P.; Pansini, M.; Colella, C. Cation exchange reactions of a sedimentary chabazite. *Micropor. Mesopor. Mat.* **1998**, *20*, 119–127. [CrossRef]
35. Rivera-Garza, M.; Olguín, M.T.; García-Sosa, I.; Alcántara, D.; Rodríguez-Fuente, G. Silver supported on natural Mexican zeolite as an antibacterial material. *Microp. Mesopor. Mat.* **2000**, *39*, 431–444. [CrossRef]
36. Demirci, S.; Ustaoğlu, Z.; Yılmazer, G.A.; Sahin, F.; Baç, N. Antimicrobial properties of zeolite-X and zeolite-A ion-exchanged with silver, copper, and zinc against a broad range of microorganisms. *Appl. Biochem. Biotechnol.* **2014**, *172*, 1652–1662. [CrossRef] [PubMed]
37. Lalueza, P.; Monzón, M.; Arruebo, M.; Santamaría, J. Bactericidal effects of different silver-containing materials. *Mater. Res. Bull.* **2011**, *46*, 2070–2076. [CrossRef]
38. Yao, G.; Lei, J.; Zhang, W.; Yu, C.; Sun, Z.; Zheng, S.; Komarneni, S. Antimicrobial activity of X zeolite exchanged with Cu^{2+} and Zn^{2+} on *Escherichia coli* and *Staphylococcus aureus*. *Environ. Sci. Pollut. Res. Int.* **2019**, *26*, 2782–2793. [CrossRef]
39. Tsitsishvili, V.; Panayotova, M.; Miyamoto, M.; Dolaberidze, N.; Mirdzveli, N.; Nijaradze, M.; Amiridze, Z.; Klarjeishvili, N.; Khutsishvili, B.; Dzhakipbekova, N.; et al. Characterization of Georgian, Kazakh and Armenian natural heulandite-clinoptilolites. *Bull. Georg. Natl. Acad. Sci.* **2022**, *16*, 39–46. Available online: http://science.org.ge/bnas/vol-16-4.html (accessed on 1 March 2023).
40. Cakicioglu-Ozkan, F.; Ulku, S. The effect of HCl treatment on water vapor adsorption characteristics of clinoptilolite rich natural zeolite. *Micropor. Mesopor. Mat.* **2005**, *77*, 47–53. [CrossRef]
41. Çakicioğlu-Özkan, F.; Becer, M. Effect of the acid type on the natural zeolite structure. *J. Turk. Chem. Soc. Sect. B* **2019**, *2*, 69–74. Available online: https://dergipark.org.tr/tr/download/article-file/738982 (accessed on 1 March 2023).
42. Yamaka, S.; Malla, P.B.; Komarnani, S. Water sorption and desorption isotherms of some naturally occurring zeolites'. *Zeolites* **1989**, *9*, 18–22. [CrossRef]
43. Simonot-Grange, M.; Elm'Chaouri, A.; Weber, G.; Dufresne, P.; Raatz, F.; Joly, J. Characterization of the dealumination effect into H faujasites by adsorption: Part 1. The water molecule as a structural aluminum ion selective probe. *Zeolites* **1992**, *12*, 155–159. [CrossRef]
44. Sano, T.; Yamanhita, N.; Iwami, Y.; Takeda, K.; Kawakami, Y. Estimation of dealumination rate of ZSM-5 zeolite by adsorption of water vapor. *Zeolites* **1996**, *16*, 258–264. [CrossRef]
45. Olson, D.H.; Haag, W.O.; Borghard, W.S. Use of water as a probe of zeolitic properties: Interaction of water with HZSM-5′. *Micropor. Mesopor. Mater.* **2000**, *35/36*, 435–446. [CrossRef]
46. Persson, I. Hydrated metal ions in aqueous solution: How regular are their structures? *Pure Appl. Chem.* **2010**, *82*, 1901–1917. [CrossRef]
47. Top, A.; Ülkü, S. Silver, zinc, and copper exchange in Na-clinoptilolite and resulting effect on antibacterial activity. *App. Clay Sci.* **2004**, *27*, 13–19. [CrossRef]
48. Adinehvand, J.; Shokuhi Rad, A.; Tehrani, A.S. Acid-treated zeolite (clinoptilolite) and its potential to zinc removal from water sample. *Int. J. Environ. Sci. Technol.* **2016**, *13*, 2705–2712. [CrossRef]
49. Hrenovic, J.; Milenkovic, J.; Ivankovic, T.; Rajic, N. Antibacterial activity of heavy metal-loaded natural zeolite. *J. Hazard. Mater.* **2012**, *201–202*, 260–264. [CrossRef]
50. Akhigbe, L.; Ouki, S.; Saroj, D.; Min Lim, X. Silver-modified clinoptilolite for the removal of Escherichia coli and heavy metals from aqueous solutions. *Env. Sci. Pollut. Res.* **2014**, *21*, 10940–10948. [CrossRef]
51. Milenkovic, J.; Hrenovic, J.; Matijasevic, D.; Niksic, D.; Rajic, N. Bactericidal activity of Cu-, Zn-, and Ag-containing zeolites toward *Escherichia coli* isolates. *Environ. Sci. Pollut. Res.* **2017**, *24*, 20273–20281. [CrossRef]

Disclaimer/Publisher's Note: The statements, opinions and data contained in all publications are solely those of the individual author(s) and contributor(s) and not of MDPI and/or the editor(s). MDPI and/or the editor(s) disclaim responsibility for any injury to people or property resulting from any ideas, methods, instructions or products referred to in the content.